The porous medium approach applied to CFD modelling of SCR in an automotive exhaust with injection of urea droplets

Benjamin, S.F. and Roberts, C.A.

The porous medium approach applied to CFD modelling of SCR in an automotive exhaust with injection of urea droplets

S. F. BENJAMIN, C. A. ROBERTS

Automotive Engineering Applied Research Group, Coventry University, UK

ABSTRACT

The automotive industry is expected to adopt SCR after-treatment to control NOx emissions from Diesel passenger cars from 2010. Ammonia promotes NOx reduction and is introduced into the exhaust as a spray of aqueous urea droplets. This is a new aspect of CFD modelling of exhaust after-treatment. When modelling sprays the mesh must be 3D and so the porous medium approach is appropriate, circumventing the need for representative single channel modelling. The porous medium technique is well established for modelling three-way catalysis and its application to SCR is demonstrated in this paper, using a kinetic scheme available in the literature. Laboratory measurements of droplet diameters have been used to specify the input of aqueous urea to the CFD model. Representative droplet parcels are modelled using a Lagrangian model within the CFD code. In this way it is possible to fully model SCR in a 3D model of an automotive catalyst system.

NOTATION

A_V	geometric surface area per unit reactor volume (m^2/m^3)
A_{PM}	catalyst precious metal surface area per unit reactor volume (m^2/m^3)
C	mass fraction
$C_{i\,g}$	mass fraction of species i in the gas phase
$C_{i\,sol}$	mass fraction of species i in the solid phase or washcoat pores
D	species diffusivity (m^2 /s)
D_d	droplet diameter (microns)
K_{mi}	mass transfer coefficient (m/s)
L	channel length, monolith length (m)
M_i	molar mass for species i (kg /mol)
ΔP	pressure drop (Pa)
P_{O2}	oxygen concentration mole fraction
q	fit variable for Rosin-Rammler droplet size distribution
Q	fraction of total volume in drops with diameter < D_d
R_i	rate of production of species i by reaction (mol /s /m^3 reactor)
t	time (s)

T	temperature (K)
U	velocity (m/s)
U_C	velocity in substrate channel (m/s)
U_S	superficial velocity for the porous medium, εU_C (m/s)
V_w	solid phase pore volume per unit volume of reactor (m^3 /m^3 reactor)
x,y	coordinates
X	fit variable for Rosin-Rammler droplet size distribution
z	axial coordinate
ε	porosity of the substrate expressed as a volume fraction
μ_t	turbulent dynamic viscosity (kg/(m s))
ρ	density (kg/m^3)
σ_s	turbulent Schmidt No.
θ	fraction of surface coverage by ammonia, ammonia storage

1 INTRODUCTION

In recent years various strategies have been rapidly developed for controlling the emissions from Diesel engine exhausts, and these were reviewed by Johnson (1). The technology was regarded as at an early stage of development (2) as recently as 2003, and Johnson (1) regarded selective catalytic reduction (SCR) as a pertinent technology only for heavy duty vehicles, with lean NOx trap (LNT) and Diesel particulate filter (DPF) technology earmarked for light duty, which includes the automotive market. It now looks likely that the preferred after-treatment technology for controlling NOx emissions in the exhaust of light duty diesel vehicles will be SCR rather than the alternative LNT system. This technology will be implemented in the period up to 2010. One disadvantage of the LNT system is the need to regenerate the NOx trap periodically by running the engine rich for short periods of about 3 seconds at intervals of typically one to two minutes. This causes some NOx slippage during the regeneration period and also a fuel penalty. This is discussed in some detail by Alimin (3). There is also the requirement to use ultra low sulphur Diesel fuel with the LNT. The SCR system typically consists of two bricks, a Diesel oxidation catalyst (DOC) followed by an SCR brick. The control system is simpler than the LNT in that SCR operates continuously without the need for regeneration, but an additional agent is required to promote the catalytic reactions, usually aqueous urea that is sprayed into the exhaust. The SCR system is therefore more complex in terms of hardware and ammonia slippage must be avoided. SCR technology has been developed over the last couple of years on heavy duty systems, for example in the work done by Gekas et al. (4). Both LNT and SCR systems may additionally require a DPF to be installed upstream to minimise soot particulate levels.

Although SCR has been proven as a technology for stationary engines and plant, the need for an additional reducing agent in a passenger car could be seen as a disadvantage of this system because of storage and filling issues. The foreseen problem with the infrastructure to supply the aqueous urea is, however, gradually being overcome, particularly in Europe where SCR technology is already in use on heavy duty vehicles. There have also been some questions about the safety of the principal catalyst chosen

for SCR, vanadium. There are now, however, promising zeolite catalysts that can be used instead (5, 6).

Diesel exhaust lean after-treatment systems are expensive to develop and test and there are advantages in being able to model such systems to predict their performance. Computational fluid dynamics (CFD) modelling is particularly useful because the flow field, which in exhaust systems is complex because of packaging constraints and contrived exhaust component geometries, can be predicted. The chemistry of the catalytic reactions can be conveniently introduced into a CFD model if the porous medium approach is used to model the flow field. In this method each monolithic catalyst substrate with parallel flow channels is modelled as a porous medium that resists the flow (7). The particular challenge of modelling SCR systems is in modelling the introduction to the computational domain of the aqueous urea droplets. Making fundamental predictions of droplet formation within a nozzle is very difficult, and also dependent on the nozzle geometry. Therefore a more generally applicable semi-empirical approach is adopted. This requires the spray to be characterised by measurement of the droplet sizes and distributions just downstream of the nozzle. The drops are then modelled by the introduction of representative droplet parcels into the computational domain, where the parcels have known properties. This is similar to the work of Kim et al. (8) on a marine engine system.

In the work reported here, some measurements have been made to characterise the spray from a prototype automotive spray system, and a full 3D SCR model has been developed based on the porous medium approach. The CFD model mesh has the dimensions of an experimental exhaust system and predictions of emissions levels can be made. Emissions measurements for comparison with the model output will be available from an experimental test rig to validate the model at a later date. In this paper, the droplet parcel model is compared with spray measurements and the effect of droplet size on the emissions predictions from the full SCR system model is assessed. In this way a useful engineering tool has been devised by a new application of the porous medium modelling approach.

2 THEORY

2.1 SCR kinetic scheme

In order to model an SCR system with a CFD model it is necessary to have a kinetic scheme with rate constant values that can provide numerical values for reaction rates. Such a scheme is given by Chi et al. (9) and consists of rates for eight chemical processes. These are HCNO hydrolysis, ammonia adsorption and desorption, two alternative ammonia oxidation reactions, standard, fast and slow SCR reactions.

All the required rate constants for this scheme are given in the literature. The rates are calculated in mol/m^2/s units, so it is necessary to have an estimate of active catalyst area per m^3 of reactor in order to apply the scheme within the porous medium model. The scheme is for a vanadium catalyst. An alternative kinetic scheme for vanadium is also available in the literature (10, 11). One of the two ammonia oxidation reactions is

$$4NH_3 + 3O_2 \rightarrow 2N_2 + 6H_2O$$

The rate (mol/m^2/s) for this reaction (9) is 1.32E+07 θ exp (– 15024/T)

The rate (mol/m^3/s) for this reaction (10) is 1.1E+09 $\theta(P_{O2}/0.02)^{0.27}$ exp(– 14193/T)

where P_{O2} is oxygen mole fraction. The rates of ammonia oxidation are calculated from the two schemes (9, 10) for oxygen mole fraction of 0.07, ammonia surface coverage of 50 % and T at 550 K. If the two schemes are assumed equivalent then comparison of the calculated values for the specified conditions implies that about 533 m^2/m^3 is the catalyst active surface area. This is an unexpectedly small target area value when compared with A_v and A_{PM} surface values used in previous porous medium catalyst models (12), which are of order 10^3 and 10^4 respectively.

The standard SCR reaction is

$4NH_3 + 4NO + O_2 \rightarrow 4N_2 + 6H_2O$

The rate (mol/m^2/s) for this reaction (9) is (1/X) 2.36E+08 [NO] [NH_3] exp(–7151/T)

where X is (1 + 0.0012042 [NH_3])

Rate(mol/m^3/s) from (10) is 2.2E+08 $C_{NO}(\theta(1-\theta)/(1+7.2\theta))(P_{O2}/0.02)^{0.27}$exp(–6615/T)

The rates of the standard SCR reaction can be calculated assuming [NO] concentration to be 0.002 mol/m^3 and [NH_3] concentration to be 0.002 mol/m^3. It is clear that the calculated rate from the Chi et al. scheme (9) is directly proportional to the ammonia concentration, whereas this dependence is not present in the Tronconi scheme (10). Comparison of the calculated values from the two schemes suggests an implicit factor of 100 m^2/m^3 for active catalyst surface area if the two schemes are equivalent. This value is even smaller than that deduced above for ammonia oxidation and suggests that the two schemes are not equivalent. The Chi et al. scheme (9) for vanadium can easily be substituted in the CFD model by an improved kinetic scheme or by kinetics specifically for zeolite. Such a scheme is now available, (13).

2.2 SCR CFD methodology

Modelling of SCR requires the introduction of the urea, which provides the ammonia for the reaction scheme, usually in the form of an aqueous spray. Spray modelling using the Lagrangian approach is by definition transient and 3D. The porous medium approach (7) lends itself readily to full 3D modelling and can predict the flow field and conversion of species. The resistance of the porous medium to flow is described by the expression

$$\frac{\Delta P}{L} = -\alpha U_S^2 - \beta U_S \qquad [1]$$

where α and β are temperature dependent permeability coefficients for the porous medium. High values of α and β disallow flow at right angles to the axis of the porous medium block. A monolithic catalyst, where the flow is constrained within parallel

channels, can therefore be modelled. Note that U_S is the superficial velocity for the porous medium such that $[\rho_{air} U_S]$ equals $[\varepsilon \rho_{air} U_C]$. The flow field is solved using the usual Reynolds averaged Navier Stokes methodology in the fluid upstream and downstream of the porous medium that represents the catalyst substrate.

For the porous medium approach the CFD model has a block of cells representing the fluid inlet. This is followed by the porous medium cells, which are used to model fluid flow through the catalyst monolith. A final block of cells models the fluid outlet. An extra block of cells with the same geometry as the porous medium cell block represents the solid properties of the monolith for heat transfer to the walls and conduction in the substrate. Enthalpy exchange between porous medium (fluid) cells and solid cells is described by source terms and appropriate heat transfer coefficients. The heat conduction equation is solved in the solid cell blocks and an effective radial thermal conductivity describes heat conduction transversely across the monolith. If the axial thermal conductivity is significantly greater than the radial value, then this can be accounted for between adjacent cells in user subroutines by an additional source term.

The general conservation equation for the transport of chemical species is shown in its full 3D version in [2] below, where the species source has units $kg/m^3/s$.

$$\frac{\partial (\rho C)}{\partial t} + \nabla \bullet (\rho U C) - \nabla \bullet \left[\left[\frac{\mu_t}{\sigma_s} + \rho D \right] \nabla C \right] = \text{Source} \qquad [2]$$

The model applies modified forms of this equation to gas phase scalars in the fluid and to either gas or solid phase scalars in the porous medium. The transient term is always included. The convective term is excluded for solid phase scalars, but retained for gas phase scalars. The diffusion flux term only applies to gas phase scalars in the fluid. The diffusion flux along the porous medium is insignificant when compared with the convective flux. The source term applies to both gas and solid phase scalars in the porous medium. It describes the net effect of diffusion of species between the gas stream and the washcoat pores on the channel wall, i.e. the solid phase, as a mass transfer process. Hence the source term replaces the diffusion flux term between gas and wall. The source is calculated using a mass transfer coefficient derived from the thin film approximation. Further details of this approach are given in (7).

The modelling methodology requires that both the gas phase and solid phase species concentrations are properties of the porous fluid cells, since only the heat conduction equation with its heat transfer source term is solved for the solid cells. Generally, species sink from the gas phase and transfer to the solid phase. The net effect of the chemical reactions, however, is often that species sink from the solid phase in a catalyst system, although for some species the reactions provide a source in the solid phase. Equations [3] to [6] presented below are laid out to clarify the requirement for inclusion of the porous medium porosity, ε. A review article by Depcik et al. (14) mentions an apparent void fraction discrepancy in the history of catalyst modelling. In the CFD model here, the monolith axis is aligned in the z direction and there is no convection of species in the x and y directions in the porous medium. The equations below are presented in 1D form for clarity.

Equation [2] applied to an element of air in a monolith channel, with the diffusion flux term replaced by a source term, kg/s/m^3 air in channel, is written as [3].

$$\frac{\partial}{\partial t}[\rho_{air} C_{i\,g}] + \frac{\partial}{\partial z}[\rho_{air} U_C C_{i\,g}] = -K_{mi} \rho_{air} \frac{A_V}{\varepsilon} [C_{i\,g} - C_{i\,sol}] \qquad [3]$$

In [3] A_V/ε is active surface area per unit volume of air in the channel. For the gas phase species in the porous medium computational cell that represents the bulk monolith, equation [4] below is solved. The term on the RHS of [4] is the source term coded into the user subroutine.

$$\varepsilon \frac{\partial}{\partial t}[\rho_{air} C_{i\,g}] + \frac{\partial}{\partial z}[\rho_{air} U_S C_{i\,g}] = -K_{mi} \rho_{air} A_v [C_{i\,g} - C_{i\,sol}] \qquad [4]$$

Typically, the catalyst washcoat occupies about 10 % of the whole monolith reactor volume and the pores in the washcoat occupy about 50% of the washcoat volume. Thus only about 1/20 of the reactor volume is available in the solid phase. Equation [2] applied to an element of air inside a pore in the catalyst washcoat at the channel surface, with the diffusion flux and convective terms suppressed, is written as equation [5], where the source term has units kg/s/m^3 air in the washcoat pore.

$$\frac{\partial}{\partial t}[\rho_{air} C_{i\,sol}] = K_{mi} \rho_{air} \frac{A_V}{V_w} [C_{i\,g} - C_{i\,sol}] + M_i \frac{R_i}{V_w} \qquad [5]$$

In [5] A_V/V_w is active area per unit volume of air in the pore and R_i / V_w is the net reaction rate for species i per unit volume of the pore. Equation [6] below is solved by the CFD solver. This enables the species concentration in the pore, i.e. in the solid phase, to be obtained in the porous medium computational cell that represents the bulk monolith. The source term on the RHS of [6] is coded into the user subroutine.

$$\varepsilon \frac{\partial}{\partial t}[\rho_{air} C_{i\,sol}] = \{K_{mi} \rho_{air} A_v [C_{i\,g} - C_{i\,sol}] + M_i R_i\} [\varepsilon / V_w] \qquad [6]$$

With the source terms coded into the CFD model via user subroutines, the transport equations are solved to provide values for the mass fractions of species in the exhaust stream.

The 3D mesh for the SCR CFD model is shown in Figure 1 and has 110016 cells in total. Droplet parcels are injected at Z 27 mm. The slow, approximately 10 degrees, expansion cone replicates the geometry of an experimental exhaust on an engine test rig. The porous medium cells represent the SCR brick and the corresponding solid cells are a separate cylindrical block of 23040 cells. A block of fluid cells downstream of the porous medium completes the mesh. Another model consisting of a simple rectangular block mesh of 80 by 80 by 250 cells was used to separately investigate the functioning of the droplet spray model. The inlet duct is 50 mm in diameter and the catalyst brick is 118 mm in diameter. The catalyst brick is 182 mm in length.

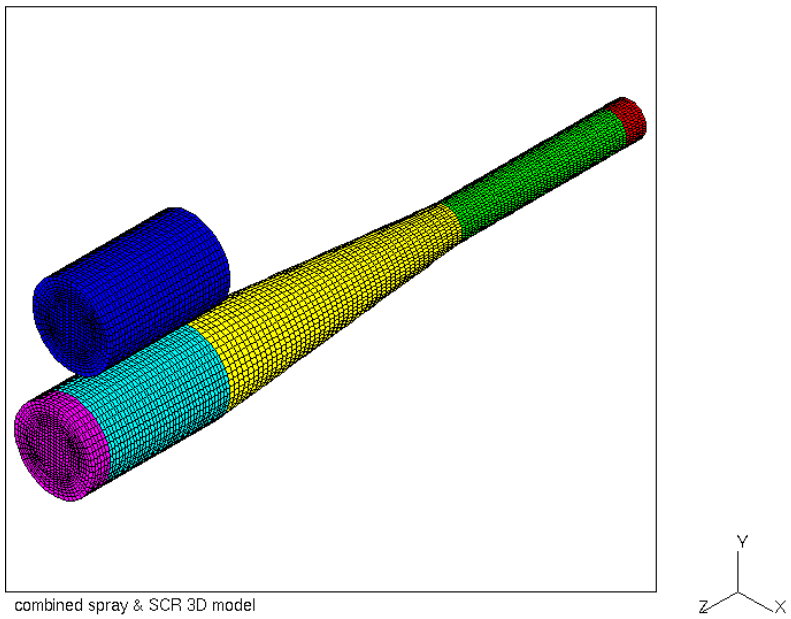

Figure 1
3D mesh for SCR CFD model. The slow expansion cone replicates the geometry of a test rig and ducts the exhaust into the porous medium. The separate cylindrical block of cells models the solid properties of the porous medium cells.

The commercial CFD package Star-CD Version 3.26 was used for the studies described in this paper. The models were run on a 16 node Itanium-2 64-bit cluster under HP-UX. The rectangular block mesh for the droplet model studies was partitioned into 4 sets for parallel runs and the SCR model mesh, shown in Figure 1, was partitioned into 10 sets for parallel runs. When using the porous medium technique it is always necessary to keep together corresponding fluid and solid cells in the same partitioned set.

2.3 Droplet sub-model methodology

The urea spray droplets enter the domain. The water is driven off as the droplet temperature approaches 373 K, leaving solid or semi-molten urea spheres. At droplet temperatures of about 410 K these should sublime or vapourise to produce gaseous urea that rapidly dissociates.

$$CO(NH_2)_2 \rightarrow NH_3 + HCNO$$

The HCNO, produced by dissociation, hydrolyses with the excess of water present in the exhaust flow and spray; this is included in the kinetic scheme. Each HCNO mol reacts to produce one mol of ammonia so that each mol of urea ultimately supplies 2 mol of ammonia (15).

The urea is introduced into the domain in the rig with an air assisted spray unit. In order to avoid the need to fully model droplet formation in the nozzle, the model uses discrete parcel input. For example, 48 mg/s of urea spray can be modelled by 480,000 parcels/s

in short runs < 0.1 second, or by 32,000 parcels per second in longer runs, for example 3 seconds. It is necessary to control the total number of droplet parcels to facilitate sufficiently rapid and convenient processing of the model output. Each parcel has mass in the range 0.1 to 1 μg but represents many individual droplets. CFD simulation time steps are arranged so that a few parcels enter per time step. Parcels are specified to the CFD package by size or size distribution, injection direction, mass flow rate and orifice size. The latter two parameters together fix the injection velocity. Also, the spray cone angle is specified. It has been found beneficial to partition the spray into five or six zones, see Figure 2, and to choose the parameter values for each zone to contour the spray to achieve predictions that compare favourably with measurements of a cold spray in a cold flow air. The real spray has a single orifice and the model has a single point of injection. Also, it was found necessary to a use a fluid source in the model to simulate the air assist to the prototype spray; it was not possible to model the detail of the behaviour of the spray by parcel injection alone. Although in reality the air assist air flow was choked, it was found that using a lower injection velocity but with the source having flux of the correct magnitude injected into a single mesh cell gave good agreement with measurements, as discussed in section 3.1. The cells in the vicinity of the air injection were refined but the dimension across the source cell was larger than the real nozzle orifice diameter.

The droplet model assumed rebound from the wall for any droplet impinging on the wall and neglected any effects of droplet collision. The geometry of the real system was such that the fairly narrow spray, 20 to 25 degrees angle, did not impinge on the wall of the duct within the computational domain when there was a surrounding air flow.

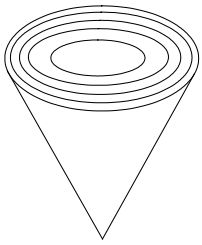

Figure 2
Schematic diagram of spray cone shown with five zones, with each annulus and the central circle having the same area.

2.4 Droplet measurements for input to CFD model

The droplets from the air-assisted prototype spray were measured by a TSI Phase Doppler Particle Anemometry (PDPA) system. This was operating in forward scatter mode. A typical droplet distribution is shown in Figure 3 for the spray discharging 48 mg/s. Data was for 30,000 valid droplets. The spray is characterised by large numbers of small droplets but small numbers of much larger droplets that contribute significantly to the volume flux. Rosin Rammler fit profiles are shown in Figure 4, indicating the uniformity of the spray when spraying into cold quiescent air. The parameters X and q given in Figure 4 are related by the standard expression

$$Q = 1 - \exp\left[\frac{-D_d}{X} \right]^q \qquad [7]$$

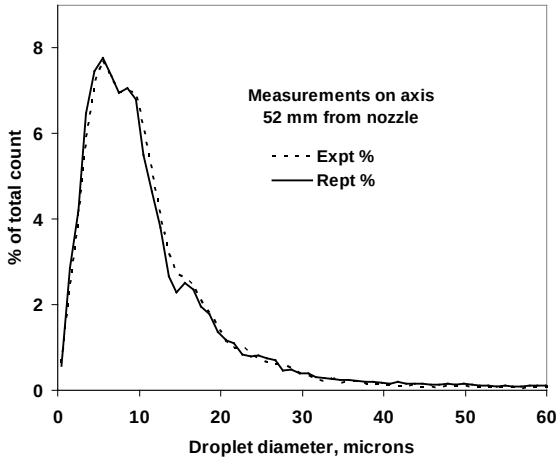

Figure 3
Typical droplet distribution. [Expt, experiment; Rept, repeat]

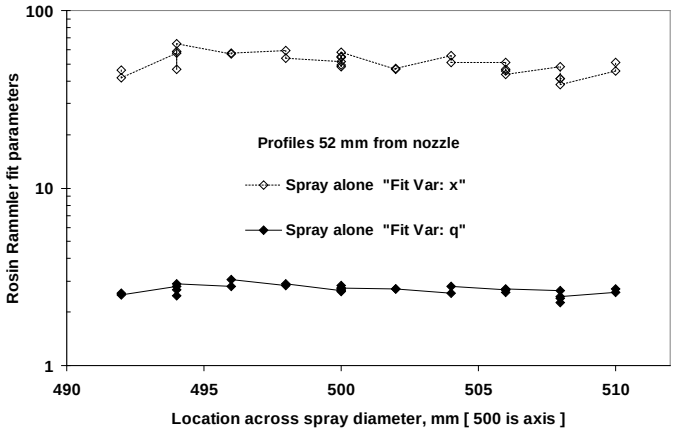

Figure 4
Profiles of Rosin Rammler fit parameters across spray spraying horizontally.

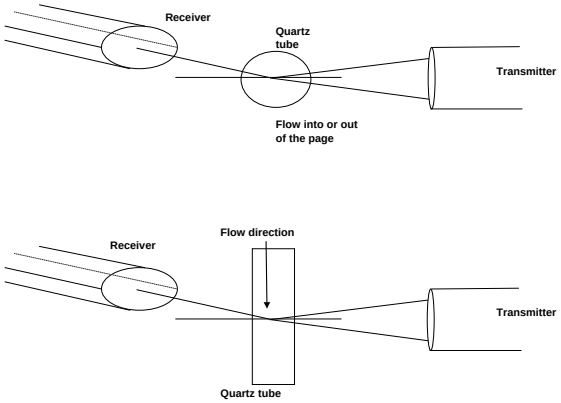

Figure 5

Alternative orientations for PDPA measurements of droplet diameters within quartz tube by forward scatter with receiver probe offset by 30 degrees.

The spray discharged through a duct of 50 mm diameter, a typical dimension for an automotive exhaust. The PDPA measurements of the spray could be made at the exit from different length tubes, either with or without additional air flow through the test rig. This technique was chosen because early measurements showed that the effects of measuring through a thin walled, 1.5 mm, quartz tube with the PDPA system were significant and attributable to refraction effects, rather than to the confining effect of tube. In the observations made by the present authors this effect could not be avoided by altering the orientation of the PDPA system relative to the tube, see Figure 5. Similar problems were anticipated even with angled plane windows. A similar effect was observed by Yimer et al. (16) who made PDPA measurements through two concentric quartz tubes of small diameters, 26 and 36 mm. Although they comment on refraction effects they seem to attribute the differences they observed in their measurements to the confining effect of the tube. In view of the uncertainty introduced by the quartz tube, the technique of using the short tubes was adopted here to circumvent the problem.

3 RESULTS FROM CFD MODELS

3.1 Injection of droplets into steady flow – comparison of CFD with data

Measurements made using the PDPA system of droplet diameters and velocities were compared with CFD predictions. The cold water spray was spraying into a steady cold air flow of about 11 m/s. The CFD simulation was run for a real time of 1.5 seconds with time steps of 0.00025 seconds. The droplet parcel injection rate to the model was 32,000 parcels/s.

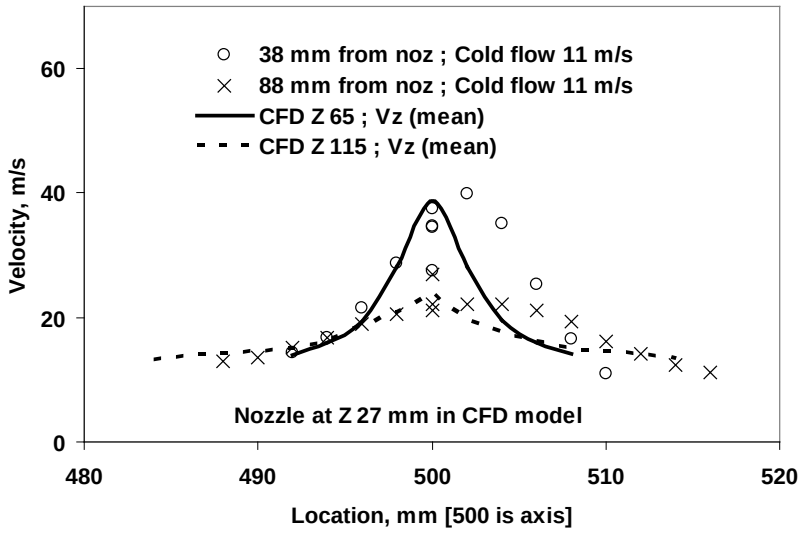

Figure 6
Droplet velocities measured and predicted across spray to show profiles.

Figure 6 shows fairly good agreement of predictions with the way that the droplet velocity profile is observed to decay in the experiments. The peak velocity falls with distance from the nozzle and the velocity falls across the spray to the surrounding air flow at the spray periphery. Figure 7 again shows the decay of the peak velocity along the axis and agreement between measurements and predictions is seen to be quite good when using a 75 m/s air injection in a single cell to model the air assist of the spray. Agreement between measurements and predictions is less good for droplet diameters in Figure 8, which shows D10 and D32 along the axis. The measurements show less change along the axis than shown by the CFD predictions. The profiles of the Sauter mean diameter in Figure 9 show good agreement on one side of the axis but fairly poor agreement on the other side. This is believed to be a feature of the prototype spray itself. The droplet CFD model developed from these simple measurements and CFD simulations was then applied to a full system SCR model.

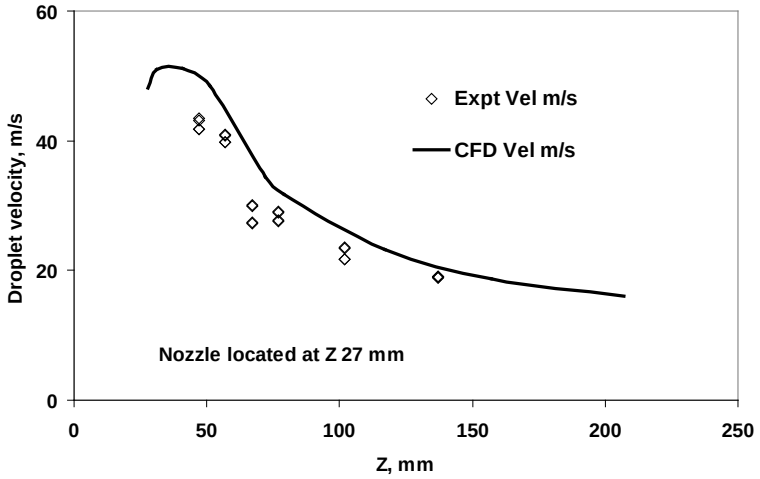

Figure 7
Mean droplet velocity along the axis for the spray through a tube with a surrounding 11 m/s air flow.

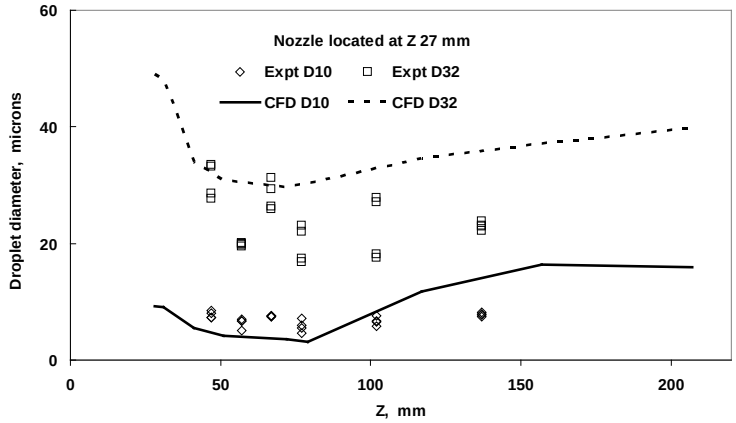

Figure 8

Comparison of drop diameter measurements with predictions.

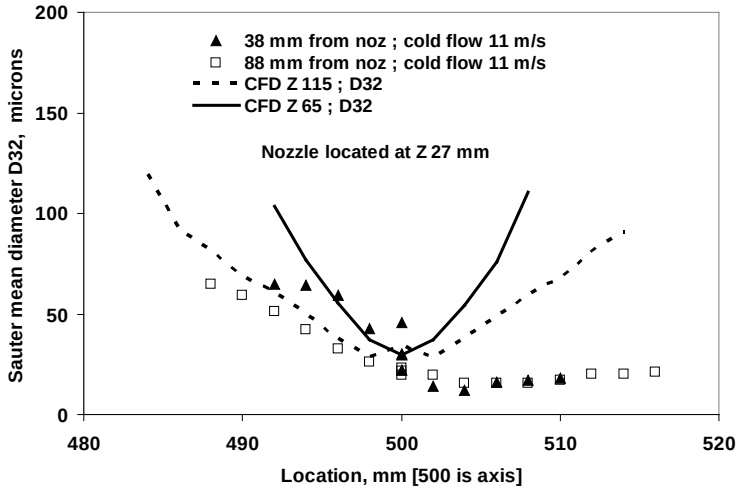

Figure 9
Sauter mean diameter profiles for droplets measured in 11 m/s cold flow, compared with CFD predictions.

3.2 Full model feasibility study

A full model simulation was carried out. This was a transient simulation that was run for 3 seconds of real time. The inlet flow was 25 m/s at 580 K. The inlet NO mass fraction was 0.00042 and the inlet NO_2 mass fraction was 0.00032. The inlet O_2 mass fraction was 9%. The inlet amount of aqueous urea was 48 mg/s entered as 20,000 droplet parcels per second. The Rosin Rammler fit parameters used to describe the spray were based on the measurements described in 3.1. The simulation took 50 hours of cpu time. The case was run in parallel across 10 processors.

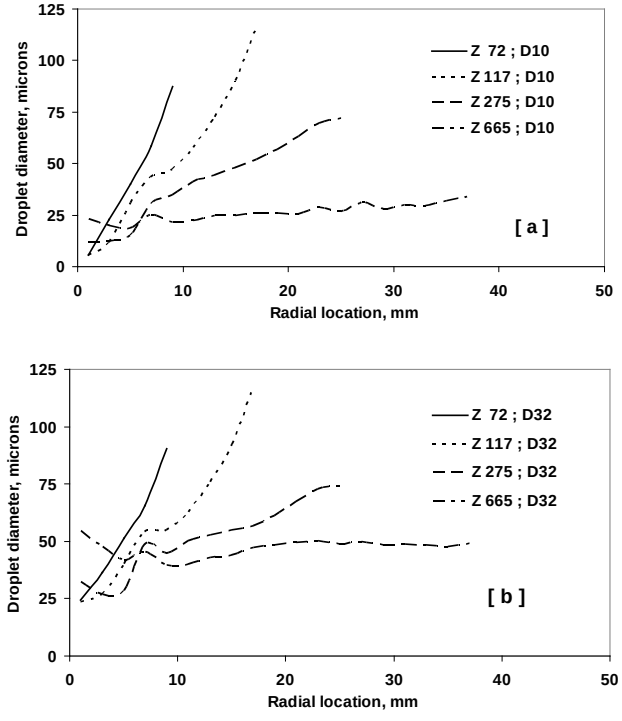

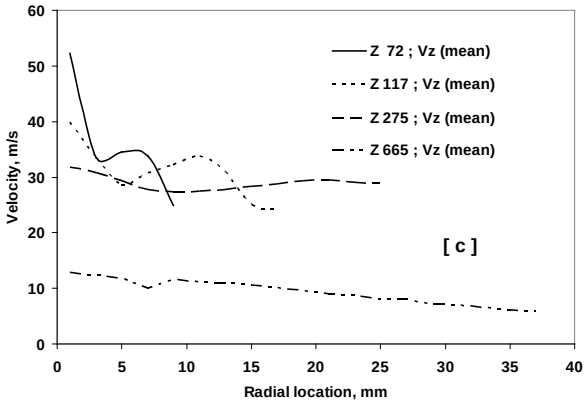

Figure 10
(a) Predicted droplet diameters, D10, (b) predicted diameters, D32, and (c) predicted velocities at four different axial locations in the full CFD model.

Figures 10 shows predictions for Z 72 and 117 mm, that is 45 and 90 mm from the droplet injection point, and also for Z 275 and 665 mm. These locations are just before the expansion cone and just before the catalyst. The model suggests fairly uniform droplet diameters and velocities at entry to catalyst, but the catalyst is 118 mm in diameter and no droplets are predicted to reach the periphery. Few droplets are found beyond 35 mm radius in the simulation. Figure 11 shows the predicted flow velocity at the exit from the SCR catalyst. The slow expansion cone, see Figure 1, has flattened the velocity profile but has not achieved a completely uniform profile.

The consequence of the spray distribution is fairly poor NOx conversion at the periphery, see Figure 12. The NOx levels in Figure 12 are shown as mass fractions; hence the velocity profile in Figure 11 determines the NOx mass flow rate profiles. The ammonia distribution is also seen in Figure 12 to be non uniform at entry to the catalyst, with negligible levels at the exit from the brick**.** This suggests that the spray spatial distribution is not sufficiently uniform and that the amount of aqueous urea input to the model is too low.

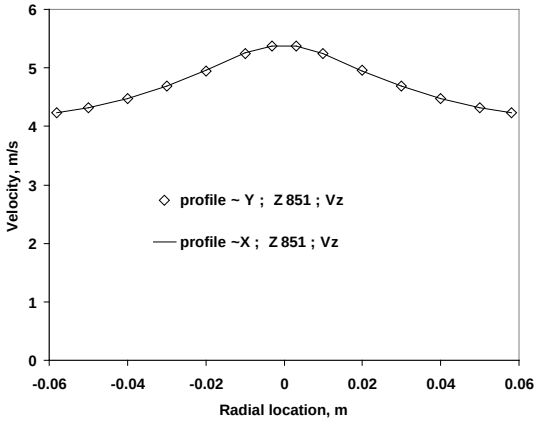

Figure 11
Predicted air velocity at Z 851 mm, the exit from the SCR catalyst in the full CFD model.

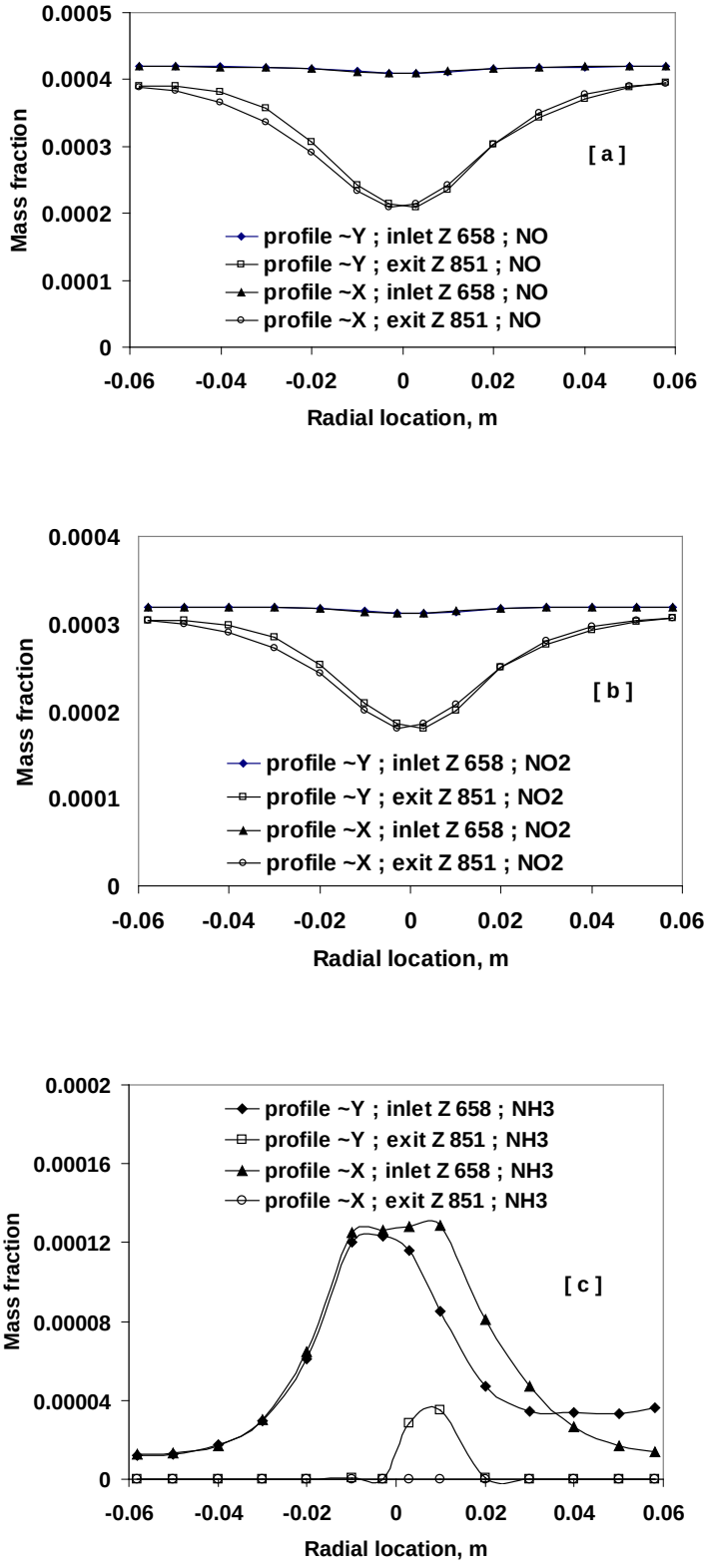

Figure 12
(a) Predicted NO, (b) predicted NO_2 and(c) predicted NH_3 profiles at inlet (Z 658 mm) and outlet (Z 851 mm) of SCR catalyst, along both X and Y axes.

4 SUMMARY OF RESULTS AND CONCLUSIONS

This paper has presented the results of droplet measurements using a phase Doppler particle anemometry system to measure both droplet diameter and velocity. The measurements were made at the exit from various length tubes to avoid the need to measure through quartz, which can introduce uncertainty into the measurements. The droplets were found to have mean diameter D10 less than 20 microns but the diameter varied across the spray profile so that larger droplets were at the edge of the spray field. The Sauter mean diameter D32 was about 30 microns on the axis but considerably larger, more than 60 microns, away from the axis. The CFD model was shown to be able to predict the droplet diameters and velocities at various distances from the nozzle. Both the change in droplet size along the axis and profiles at different distances from the axis were measured and predicted satisfactorily.

The porous medium approach can be used to model SCR catalysis in an automotive exhaust context. The spray model validated against PDPA measurements in cold flow studies was incorporated into the full SCR model. A kinetic scheme from the literature was evaluated and applied within the model. The results demonstrate the feasibility of the methodology, which incorporates a droplet sub-model into a model based on the porous medium approach. The output from the model indicates the limitations of the spray investigated here as a means of introduction of ammonia. They show that this spray is probably of too narrow an angle, and insufficiently well mixed and that the amount of urea injected is too low in the simulation. The spray angle and droplet size both influence how well the droplets convert to ammonia in the real exhaust system.

The work described here has been extended to an alternative spray and will ultimately be tested against species measurements in an engine exhaust. Matching the amount of urea injected to the levels of NOx in the exhaust is an ongoing challenge, particularly under transient conditions, but a validated CFD model is a useful tool in assisting further developments.

ACKNOWLEDGEMENTS

Technical and financial support from Jaguar-LandRover, EMCON Technologies and Johnson Matthey is gratefully acknowledged.

REFERENCE LIST

1. Johnson, T. V. Diesel emission control in review – the last 12 months. SAE paper No. 2003-01-0039. Also published in Diesel Exhaust Emissions Control, SAE SP-1754

2. Twigg, M. V. Automotive exhaust emissions control. Platinum metals Rev. Vol. 47 (4) (2003) pp 157 – 162

3. Alimin, A. J. Experimental investigation of a NOx trap using fast response emission analysers. PhD thesis, Coventry University, UK, 2006

4. Gekas, I., Gabrielsson, P., Johansen, K. Urea-SCR catalyst system selection for fuel and PM optimized engines and a demonstration of a novel urea injection system. SAE paper No. 2002-01-0289

5. Baik, J. H., Yim, S. D., Nam, I-S., et al. Control of NOx emissions from diesel engine by selective catalytic reduction (SCR) with urea. Topics in Catalysis. Vols 30/31 (July 2004) pp 37 – 41

6. Li, G., Jones, C. A., Grassian, V. H., Larsen, S.C. Selective catalytic reduction of NO2 with urea in nanocrystalline NaY zeolite. Journal of Catalysis Vol. 234 (2005) pp 401 – 413

7. Benjamin, S. F., Roberts, C. A. Three-dimensional modelling of NOx and particulate traps using CFD: A porous medium approach. Applied Mathematical Modelling Vol. 31 (2007) pp 2446 – 2460

8. Kim, J. Y., Ryu, S. H., Ha, J. S. Numerical prediction on the characteristics of spray-induced mixing and thermal decomposition of urea solution in SCR system. Proceedings of ICEF04, 2004 Fall Technical Conference of ASME Internal Combustion Engine Division. Paper No. ICEF2004-889

9. Chi, J. N., Dacosta, H. F. M. Modelling and control of a urea-SCR after treatment system. SAE Paper No. 2005-01-0966

10. Chatterjee, D., Burkhardt, T., Bandl-Konrad, B., et al. Numerical application of ammonia SCR catalytic converters: Model development and application. SAE Paper No. 2005-01-0965

11. Tronconi, E., Nova, I., Ciardelli, C., et al. Modelling of an SCR catalytic converter for diesel exhaust after-treatment: Dynamic effects at low temperature. Catalysis Today Vol. 105 (2005) pp 529 – 536

12. Benjamin, S. F., Roberts, C. A. Automotive catalyst warm up to light off by pulsating engine exhaust. Int J Eng Res Vol. 5 No. 2 (2004) pp 125 – 147

13. Chatterjee, D., Burkhardt, T., Weibul, M., et al. Numerical simulation of Zeolite and V-based SCR catalytic converters. SAE Paper No. 2007-01-1136

14. Depcik, C., Assanis, D. One-dimensional automotive catalyst modelling. Progress in Energy and Combustion Science. Vol. 31 (2005) pp 308 – 369

15. Yim, S. D., Kim, S. J., Baik, J. H. Decomposition of urea into NH3 for the SCR process. Ind Eng Chem Res Vol. 43 (2004) pp 4856 – 4863

16. Yimer, I., Jiamg, L. Y., Campbell, I., et al. Combustion noise reduction in a kerosene burner: Investigations in the spray characteristics of the fuel nozzle. National Research Council of Canada Report NRCC-47050. Also published in Combustion Institute Canadian Section Spring Technical Meeting, May 2004